

4.2.4.2 Photoelastic Data Analysis

Figures 4.17 and 4.18 present the isoclinic angle analysis from photoelastic images I_3 through I_6 . As described in Chapter 3, the rotational alignment of the polarization optics relative to the first polarizer has a prominent effect on the wrapped isoclinic angle data. Figures 4.17(a)–4.17(b) show how the isoclinic angle measurement is sensitive to errors in the polarization alignment, particularly to the misalignment of the first $\lambda/4$ plate, resulting in false discontinuities and regions that incorrectly sweep through zero. These features, which are near regions where $\sin(\delta) = 0$, are not apparent in the theoretical wrapped isoclinic angle from well-aligned optics in Figure 4.17(d). The theoretical field in Figure 4.17(b) incorporates a small misalignment in the first $\lambda/4$ plate of $\pi/180$ from the ideal position of $\xi = \pi/4$, resulting in similar error features as the experimental field in Figure 4.17(a).

The false discontinuities and regions that incorrectly sweep through zero are corrected manually, as outlined in Section 3.2.4.1, focusing on regions near $\sin(\delta) = 0$ and the viewing the ambiguous wrapped isochromatic phase generated from the wrapped isoclinic angle, given in Figure 4.17(e). Regions in wrapped δ that correspond to phase ambiguities, obvious in the theoretical ambiguous wrapped δ along lines near $\theta = \pm 2\pi/3$ in Figure 4.17(f), should correspond to real $\pi/2$ discontinuities in the wrapped α that will require unwrapping later, like those near $\theta = \pm 2\pi/3$ in Figure 4.17(d). False $\pi/2$ discontinuities in α lie where the ambiguous wrapped δ has good modulation, often near $\sin(\delta) = 0$, such as near the lower parts of the lobes around $x = 0.25$ mm in Figure 4.17(e); these false α discontinuities are interpolated across to remove the discontinuities. Regions in the wrapped α where the angle sweeps through zero but corresponds to ambiguous wrapped δ or near broken 2π δ discontinuities, such as on the upper parts of the lobes around $x = -0.5$ mm in Figure 4.17(e), require careful consideration; a $\pi/2$ discontinuity is added to these regions, and the surrounding data is smoothed appropriately.

All of these manual changes of the wrapped isoclinic angle are guided by some basic *a priori* knowledge of the general trend of α , keeping in mind that α does not often have large gradients, though the 2D asymptotic crack problem is unusual with a large gradient across the crack plane. The crack problem is ideally radially symmetric, so the phase discontinuities should be radial in nature.

The corrected wrapped α in Figure 4.17(c) is close to this expectation, with slightly more variance from radial symmetry near the interpolated regions near the crack tip. The corrected wrapped α in Figure 4.17(c) unwraps well, as shown in comparing the experimental and theoretical values in Figures 4.18(a)–4.18(b) with the largest errors near regions where $\sin(\delta) = 0$. The experimental α does not capture the large jump near $\theta = 0$, but moves continuously through that region, evident in the line plot of the theoretical and experimental wrapped and unwrapped α at $x = 1.10$ mm in Figure 4.18(c). Since $\sin(\delta)$ is close to zero in this region, the $\lambda/4$ plate error causes false discontinuities emanating from the crack tip radially, as shown in Figures 4.17(a) and 4.17(b). This affected region obscures the large jump in α near $\theta = 0$. From the guidelines stated above for correcting the wrapped α , the discontinuities near $\theta = 0$ appear, upon first consideration, to be real discontinuities with their radial behavior and their correspondence to ambiguous wrapped δ . The only indication that these might be false discontinuities is that these are near regions with $\sin(\delta) = 0$. Corrections to such discontinuities to mimic the theoretical wrapped data would be difficult without knowing the *exact* behavior of α , which is not possible without knowing K_I and K_{II} that are calculated after the phase analysis is complete. Fortunately, the false discontinuities in this case lead to unwrapped α that loosely approximates the theoretical α in these Mode I–dominant fracture cases, evident in Figure 4.18(c), such that the subsequent isochromatic data appears to be reasonable, as discussed below; thus, these particular false discontinuities are not modified.

Figure 4.19 shows the experimental and theoretical wrapped and unwrapped isochromatic phase with excellent agreement globally. Both experimental and theoretical fields are slightly rotated in the $-\theta$ direction due to the slight Mode II component, have similar lobe shapes, and have similar locations for the 2π phase discontinuities in the wrapped phase. Due to the slight error in the isoclinic angle near $\theta = 0$, the experimental field does not reach to the low values close to zero as the theoretical field does in this region, but the general trend of smaller phase values does hold.

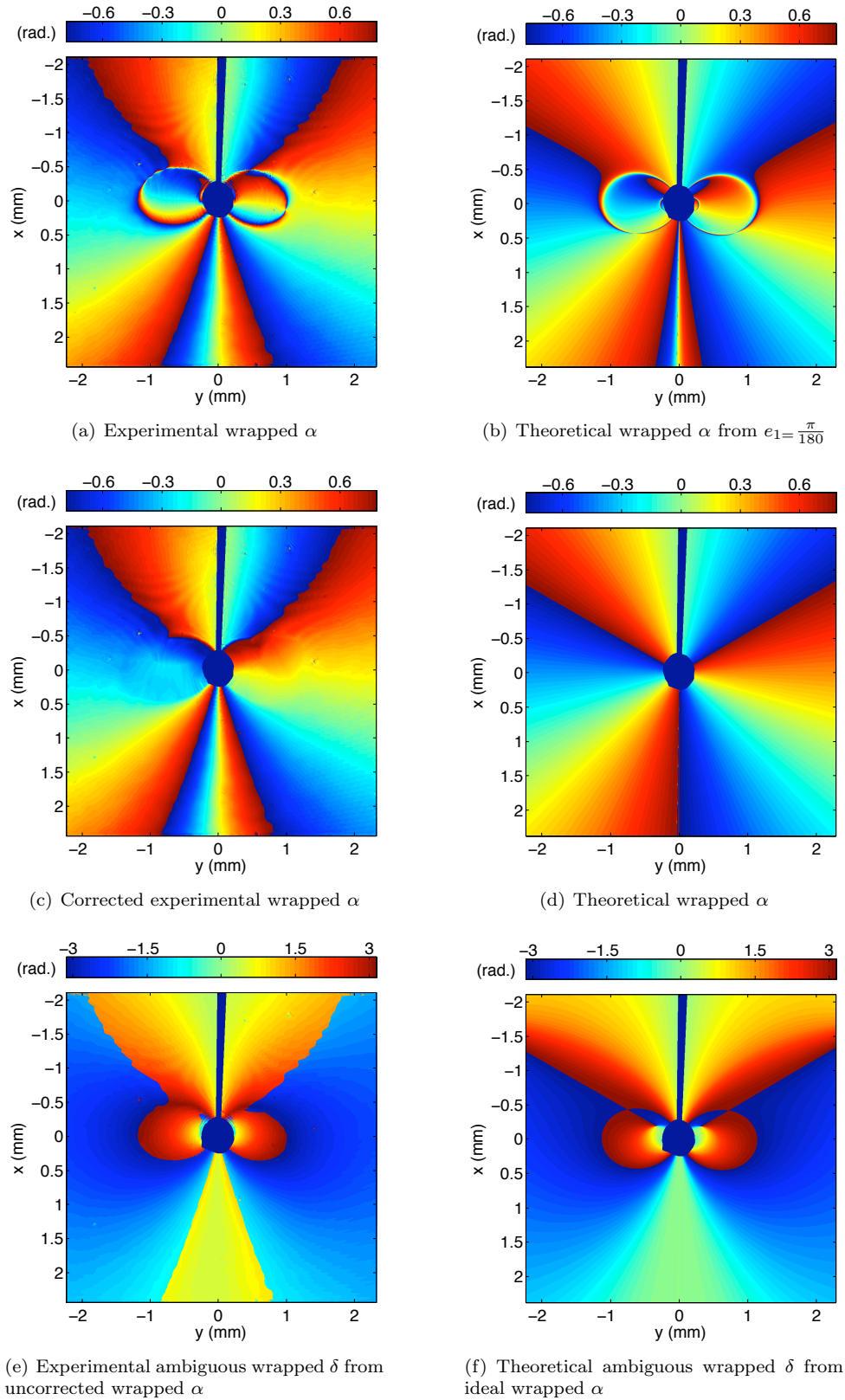


Figure 4.17: Experimental and theoretical data for the isoclinic angle for specimen HomC1 for $K_I = 0.514 \text{ MPa}\sqrt{\text{m}}$ and $K_{II} = 4.4 \text{ kPa}\sqrt{\text{m}}$ with crack region masked in blue

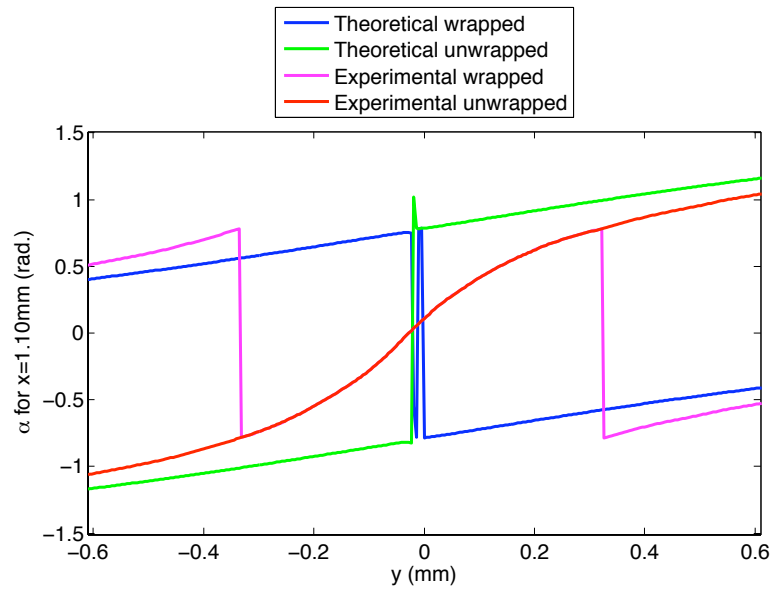
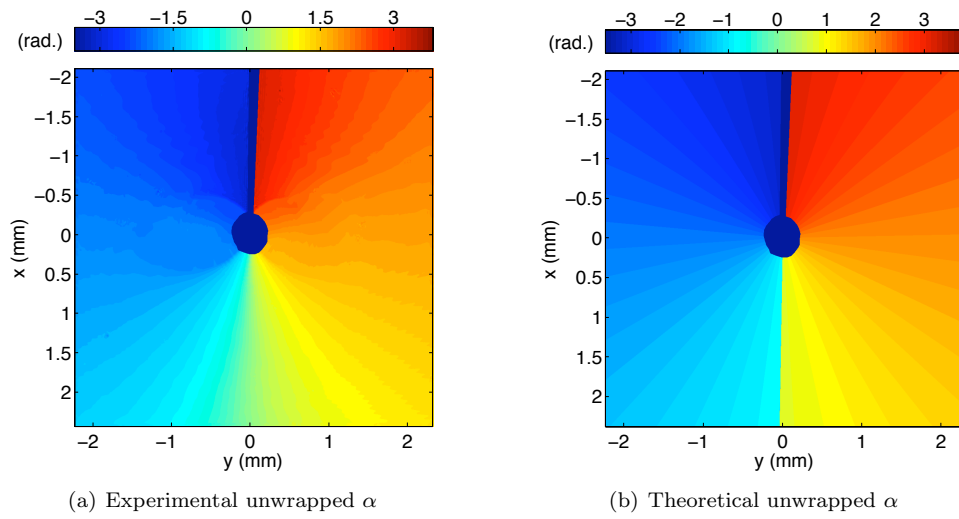


Figure 4.18: Experimental and theoretical unwrapped isoclinic angle with crack region masked in blue and comparison of experimental and theoretical wrapped and unwrapped α for $x = 1.10$ mm

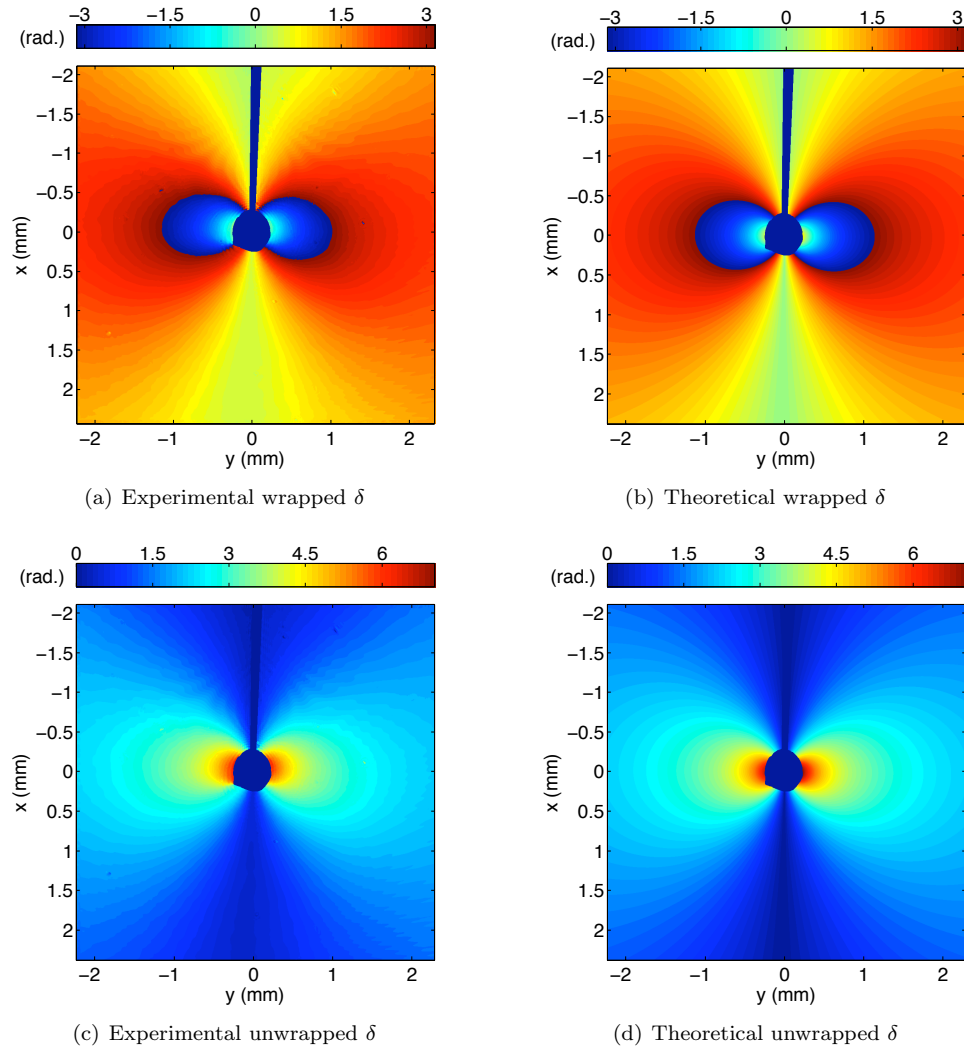


Figure 4.19: Experimental and theoretical data for the isochromatic phase for specimen HomC1 for $K_I = 0.514 \text{ MPa}\sqrt{\text{m}}$ and $K_{II} = 4.4 \text{ kPa}\sqrt{\text{m}}$ with crack region masked in blue